Proton-Linked Contributions to Site-Specific Interactions of λ *c*I Repressor and O_R[†]

Donald F. Senear[‡] and Gary K. Ackers*

Department of Biology and McCollum-Pratt Institute, The Johns Hopkins University, Baltimore, Maryland 21218

Received December 6, 1989; Revised Manuscript Received February 28, 1990

ABSTRACT: The effects of proton activity on the site-specific interactions of *c*I repressors with operator sites O_R were studied by using DNase I footprint titration. Individual-site binding isotherms were obtained for the binding of repressor to each site of wild-type O_R and of mutant operators in which binding to some sites is eliminated. The Gibbs energies for binding and for cooperativity (in every operator configuration) were determined at each pH (range 5–8). The proton-linked effects clearly account for a significant fraction of the difference in affinities for the three operator sites. The most dramatic effects on the repressor–operator binding interactions are at acid pH, and therefore do not involve the basic groups in the repressor N-terminal arm known to contact the DNA. Also, the proton-linked effects are different at the three operator sites as indicated by significantly different derivative relationships, $d \ln k / d \ln a_H = \Delta \bar{\nu}_H$. These results implicate ionizable repressor groups which may not contact the DNA and conformational differences between the three repressor–operator site complexes as being important components to the mechanism of site specificity. The extensive data base generated by these studies was also used to reevaluate the traditional models used to describe cooperativity in this system. The results confirm the lack of significant cooperative interaction between O_R1 and O_R3 at all conditions. However, the data for some experimental conditions are clearly inconsistent with the (selection) rule, that cooperative interaction between O_R2 and O_R3 is eliminated by ligation at O_R1 [Johnson, A. D., Meyer, B. J., & Ptashne, M. (1979) *Proc. Natl. Acad. Sci. U.S.A. 76*, 5061–5065].

A common feature of transcriptional regulation in both prokaryotes and eukaryotes is the interaction of gene regulatory proteins with specific DNA sequences. An example, one that has served as a prototype for studies of this type of gene regulatory mechanism, is provided by the right operator (O_R)[1] of the bacteriophage λ. The interactions of the phage-encoded *c*I and *cro* repressors with the three operator sites at O_R constitute the primary control of the switch from lysogenic to lytic phases of the phage [see Ptashne (1986) for a review]. The two crucial elements to this regulation are (i) the differential affinities of *c*I and *cro* repressors for the three phage operator sites and (ii) cooperative interactions between *c*I repressor dimers bound to different operator sites (Johnson et al., 1979). A key to understanding the molecular mechanism of regulation mediated by such an assembly of interacting macromolecular components is to understand the chemical and physical basis for the macromolecular interactions. To this end, we have initiated detailed studies on the energetics of interactions between *c*I repressor and O_R in order to deduce the significant chemical forces responsible for cooperativity and site specificity.

The most popular approach to this issue has been to analyze mutations that inhibit repressor binding [cf. Hochschild et al. 1986), Nelson and Sauer (1986), and Benson et al. (1989)]. This approach focuses on amino acids and DNA bases that physically contact one another, and its interpretation usually rests on the assumption that the effects of mutation are strictly local. The recent repressor–operator, cocrystallographic structures of the λ *c*I repressor (Jordan & Pabo, 1988), of the 434 *c*I (Aggarwal et al., 1988) and *cro* (Wolberger et al., 1988) repressors, and of the *Escherichia coli* trp repressor (Otwinowski et al., 1988) have emphasized some limitations of these interpretations. By contrast, a thermodynamic approach characterizes the energetically significant interactions, regardless of the structural complexity of their origin. The development of the footprint titration technique as a quantitative method for measuring individual-site thermodynamics (Brenowitz et al., 1986a,b) extends this approach to site-specific protein–DNA regulatory assemblies. By using this method and combining data for wild-type and "reduced valency" mutant operators (Senear et al., 1986), it is possible to resolve the energetics of each macromolecular interaction, and to assess its role in the regulation of the entire assembly.

In the present study, we have used the footprint titration method to analyze the effects of proton activity of the *c*I repressor–O_R interactions from pH 8 to pH 5. At each pH, the titration data for O_R wild-type and four different mutant operators were analyzed to resolve both the Gibbs free energies for repressor binding to each of the operator sites and the additional free energies of cooperative interaction of every configuration of the operator. The pH effect was studied because of our expectation that proton absorption would

[†] This work was supported by National Institutes of Health Grants GM 24486 and GM 39343.

* Correspondence should be addressed to this author at the Department of Biochemistry and Molecular Biophysics, Washington University School of Medicine, 660 South Euclid Av., Box 8231, St. Louis, MO 63110.

[‡] Present address: Department of Molecular Biology and Biochemistry, University of California, Irvine, CA 92717.

[1] Abbreviations: DNase I, bovine pancreas deoxyribonuclease I (EC 3.1.21.1); bis(acrylamide), *N,N'*-methylenebis(acrylamide); TEMED, *N,N,N',N'*-tetramethylethylenediamine; BSA, bovine serum albumin; CT-DNA, calf thymus DNA; Tris, tris(hydroxymethyl)aminomethane; $NaDodSO_4$, sodium dodecyl sulfate; EDTA, (ethylenedinitrilo)tetraacetic acid; Bistris, [bis(2-hydroxyethyl)amino]tris(hydroxymethyl)methane; EtOH, ethanol; BRL, Bethesda Research Labs; O_R, λ right operator; bp, base pair(s).

0006-2960/90/0429-6568$02.50/0

contribute significantly to energetics of the protein–DNA binding reactions, and also to cooperativity. The repressor N-terminal domain, O_L1 cocrystal structure (Jordan & Pabo, 1988) supports the view that the detailed conformation of the DNA backbone is an important component in repressor recognition. Acid–base reactions of amino acids might be sensitive to sequence-dependent variations in DNA conformation, either directly due to variations in the electrostatic potential around the DNA or indirectly due to any conformational accommodation of repressor in binding DNA. Either would lead to differential effects at the three operator sites.

The results of these studies do indicate a significant effect of proton-linked processes on the free energies of repressor binding to the operator sites. Our results also indicate a significant contribution to the *differences* in free energy for binding to the three operator sites, hence, to the mechanism of site specificity. Surprisingly, there are only moderate effects on cooperativity, suggesting that ionizable groups may not play major roles in these interactions. Potential origins of these effects and their implications regarding the mechanism of site-specific DNA binding are discussed.

Materials and Methods

Chemical Reagents. α-^{32}P-labeled deoxyribonucleotides (3000 Ci/mmol) were purchased from Amersham; unlabeled deoxyribonucleotides were from P-L Biochemicals. Electrophoresis-grade acrylamide, bis(acrylamide), ammonium persulfate, and TEMED were supplied by Bio-Rad. Acrylamide, bis(acrylamide), and urea were deionized by using Bio-Rad AG501-X8 mixed-bed resin prior to use. Urea was sequenal grade from Pierce. CsCl used was special biochemical grade from Gallard–Schlesinger. All other reagents were reagent or analytical grade.

Biological Materials. The restriction endonucleases *Hae*III, *Hin*dIII, and *Pst*I were purchased from Bethesda Research Labs (BRL). *Bgl*II and the large (Klenow) fragment of *E. coli* DNA polymerase I were from New England Biolabs. Bovine serum albumin (BSA) was from BRL (acetylated–nucleic acid enzyme grade), and calf thymus DNA (CT-DNA) was from P-L Biochemicals. Bovine pancreas deoxyribonuclease I (DNase I, code D) from Worthington (Cooper Biomedical) was stored as a 2 mg/mL stock solution in 50 mM Tris-HCl, pH 7.2, 10 mM $MgCl_2$, 1 mM $CaCl_2$, 1 mM dithiothreitol, and 50% glycerol at −70 °C and diluted appropriately into assay buffer (see below) less BSA and CT-DNA, immediately before use. In order to obtain constant DNase I exposure over the pH range, the relative catalytic activity was determined at each pH, essentially as described (Kunitz, 1950).

The repressor protein used has beed previously described (Senear et al., 1986). It is greater than 95% pure as estimated by electrophoresis on $NaDodSO_4$, but only 79% active, based on stoichiometry experiments of the type described by Sauer (1979) and by Johnson (1980), and on $\epsilon^{280nm}_{mg/mL} = 1.18$. Total, active monomer concentrations were calculated from the stoichiometry experiments.

Preparation of Radiolabeled Operator DNA. Operator-containing DNA fragments used in these studies were derived from the following sources. Plasmids pBJ301, pBJ303, pBJ304, and pBJ306 (Meyer et al., 1980) containing the λ right operator were gifts from J. Eliason and M. Ptashne. Each contains a single base pair substitution in one or two of the operator binding sites, which eliminate (−) or reduce (r) specific repressor affinity for that site. The binding competencies of these operators are O_R1^-, $O_R1^-3^-$, $O_R1^-2^-$, and O_R2^-, respectively. O_R^+-containing plasmid pKB252 (Backman et al., 1976) and pHE6 were gifts from H. Nelson and R. Sauer and from M. Wold and R. McMacken, respectively.

Plasmids were purified by the procedure of Birnboim and Doly (1979) followed by CsCl density centrifugation (Maniatas et al., 1982) and electrophoresis on 1% agarose gels. Operator-containing fragments were excised from the plasmids with *Bgl*II (bp 38 103 in the λ *cro* gene) and either *Hin*dIII (bp 37 459), *Hae*III (bp 37 247), or *Pst*I (bp 37 001) in the λ *c*I gene, yielding fragments of 648, 861, and 1107 bp, respectively. DNA fragments were isolated by electrophoresis through 1.5% agarose gels, and purified by chromatography on NACS–prepac (BRL). The fragments were labeled with α-^{32}P-labeled deoxyribonucleotides at the *Bgl*II site by using Klenow polymerase (Maniatas et al., 1982). A high concentration of unlabeled nucleotides was added before termination of the labeling reaction to ensure that all labeled strands were the same length. The radiolabeled DNA was purified by chromatography on two 1.0-mL Sephadex G-50 spin columns (Maniatas et al., 1982), chromatography on NACS–prepac, and EtOH precipitation. The typical specific radioactivity of freshly labeled DNA [(6–9) × 10^6 Ci/mol] was used to estimate the operator concentration in binding experiments.

Individual-Site Binding Experiments. These experiments were conducted by using the quantitative DNase I footprint titration method, exactly as described previously (Brenowitz et al., 1986a). All binding experiments were conducted in a buffer (assay buffer) consisting of 10 mM Tris (pH 8.00 ± 0.01), Bistris (pH 7.00, pH 6.00), or acetate (pH 5.00), 0.200 M KCl, 2.5 mM $MgCl_2$, 1.0 mM $CaCl_2$, 0.1 mM Na_4EDTA, 100 μg/mL BSA, and 2 μg/mL CT-DNA (sonicated). Reaction mixtures were incubated in a water bath at 20 ± 0.1 °C for 1 to several h prior to binding assays. Binding measurements did not depend on incubation time over this range. Equilibrium mixtures contained 15 000–30 000 cpm of ^{32}P-labeled operator DNA in a volume of 200 or 300 μL (less than 5 pM in operator-containing fragments, below pH 7 and less than 15 pM above). Conditions for DNase I exposure were 75–450 ng of DNase I (depending upon the DNase I catalytic activity at each pH) added in a 5-μL volume, for 1.0 min. Electrophoresis on 6% or 8% acrylamide–urea denaturing gels, autoradiography, two-dimensional optical scanning, and calculation of the fractional occupancy of each of the individual operator sites were exactly as described previously (Senear et al., 1986; Brenowitz et al., 1986).

Numerical Analysis. The binding data were analyzed according to the appropriate quantitative expressions by using nonlinear least-squares methods of parameter estimation. The analysis program (Johnson & Frasier, 1985) uses a variation of the Gauss–Newton procedure (Hildebrand, 1956) to determine the best-fit, model-dependent parameter values corresponding to a minimum in the variance. The N-dimensional parameter space is searched for the variance ratio predicted by an F statistic (Box, 1960) to determine the worst case joint confidence intervals for the fitted parameters. The confidence limits correspond to approximately one standard deviation.

In the simultaneous analyses of data from different experiments, e.g., from binding experiments for wild-type and reduced valency mutant operators, weighting factors were employed to account for variations in experimental noise. To obtain the weights, each individual binding experiment was first analyzed separately to obtain the best possible "phenomenological" fit. Since binding data for single operators do not provide unique resolution of all of the Gibbs energy terms (Senear et al., 1986), different combinations of the ΔG_{ij} terms were used as fixed input parameters in these separate

analyses. ΔG_1, ΔG_2, ΔG_3, and the titration end points [see Brenowitz et al. (1986a)] were fitted parameters. The variances obtained for the best combination of ΔG_{ij} terms were taken to indicate the precision of the individual data points. These were used to calculate normalized weighting factors (Bevington, 1969) given by

$$\sigma_{ij} = N_t(1/\sigma_j^2)/\sum_j(N_j/\sigma_j^2) \quad (1)$$

where σ_{ij} is the weight assigned data point i of experiment j, σ_j^2 and N_j are the variance and number of data for experiment j, respectively, and $N_t = \sum_j N_j$.

At most experimental conditions, the operator concentration was sufficiently low to ignore the difference between unliganded and total repressor concentrations. The free dimer concentration was calculated directly from the truncated repressor conservation equation, $R_t = R_1 + 2R_2$ (in monomer units), and the dimer dissociation equilibrium constant, $k_d = R_1^2/R_2$. However, due to the extremely high affinity of repressor for O_R at pH 5, the bound repressor could not be safely ignored.

In order to analyze the pH 5 data, the full conservation equation was utilized. This is given by

$$R_t = R_1 + 2R_2 + 2O_t\sum_s f_s \quad (2)$$

where R_1, R_2, and O_t refer respectively to repressor monomer, repressor dimer, and operator concentrations and f_s is the probability of operator configuration s (Table I) with repressor stoichiometry j. The f_s terms are defined by eq 4 (see Results). Rearrangement yields 8th order polynomials in R_1 for each of the (wild-type and mutant) operators. At each iteration of the least-squares procedure, the bisector method (Johnson & Riess, 1982), the current estimates of the ΔG_i's and ΔG_{ij}'s, and the estimated operator concentration were used to obtain the only real root of the appropriate polynomial in the range $O \leq R_1 \leq R_T$, for each R_T (the experimental, independent variable). The uncertainty in estimating operator concentrations was not sufficient to significantly affect the fitted ΔG_i and ΔG_{ij} values.

Trapezoidal integration of the individual-site binding data was used to calculate individual site loading energies ($\Delta G_{l,i}$). The level of experimental noise of the data and the complex shapes of the isotherms defeated attempt to smooth the points, prior to numerical integration. The titration end points from the best "phenomenological" fits were used in the calculations. The uncertainties in the calculated values were estimated by fitting the data for each site to a noncooperative (Langmuir) binding isotherm. Analysis of simulated data with random errors introduced to the dependent variable was used to relate confidence intervals for fitted binding energies to the uncertainty in $\Delta G_{l,i}$. At all levels of Gaussian noise tested, the standard deviation of $\Delta G_{l,i}$ calculated for 100 simulated data sets was accurately refected (or overestimated) by the confidence intervals for the fitted binding energies. All calculations were performed on a Hewlett-Packard 1000 computer system.

Results

Footprint Titration Analysis of Repressor Binding to O_R. Figure 1 presents a representative titration of an O_R1^- operator. Repressor binding to O_R2 and to O_R3 is evidenced by increasing protection in those sites; by contrast, there is no protection at O_R1. Standard regions outside of the binding sites are used to normalize the protection to the amount of DNA loaded in each lane (Brenowitz et al., 1986a). High carrier DNA concentrations maintain the unliganded DNA

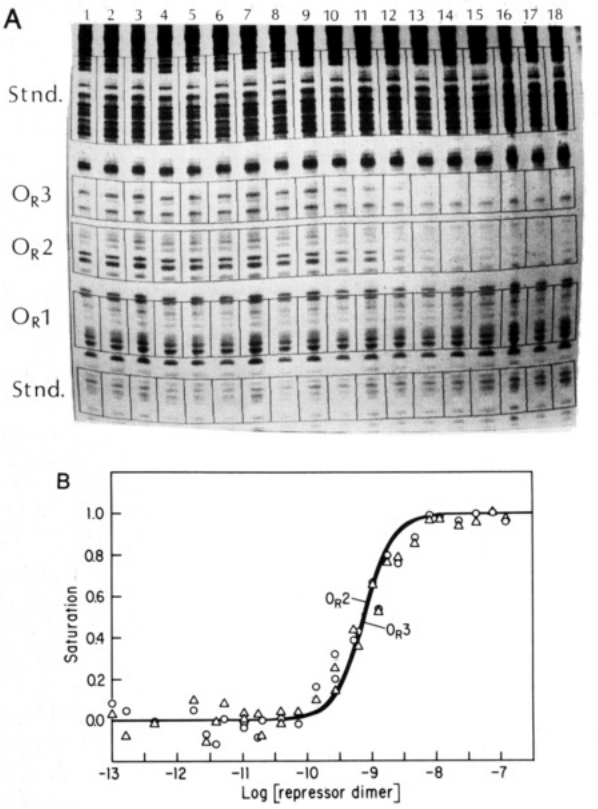

FIGURE 1: Footprint titration of *c*I repressor binding to sites O_R2 and O_R3 of an operator in which specific binding to O_R1 is eliminated (O_R1^-). Reaction conditions are 20 °C, standard assay buffer, pH 7. (A) Autoradiogram of the DNA after exposure to DNase I. Blocks of bands corresponding to the operator sites and to standards (see text) used to calculate the extent of saturation are marked. Lane 19 is a control lane showing the nicking of the labeled strand of the DNA prior to DNase I exposure. (B) Individual-site binding data. Extent of saturation for sites O_R2 (open circles) and O_R3 (open triangles) determined from the autoradiogram shown and from a companion experiment. Solid curves drawn through the points represent the simultaneous analysis of all binding data for wild-type and reduced valency operators, at this condition, as described in the text. Estimated interaction energies are in Table II.

concentration constant, even as the operator sites are filled. This avoids the overall increase in DNase nicking outside of operator sites that is observed in other systems (Ward et al., 1988). The absence of protection outside of operator sites, at every experimental condition tested, indicates that the repressor maintains its high specificity over the entire pH range, 5–8. At pH 5, repressor binding does induce "hot spots", i.e., increased DNase I nicking at the first few base pairs outside of binding sites. Appropriate choice of bands used to represent operator sites and standards obviates this artifact. This effect is observed at no other condition and might indicate either pH-dependent, repressor binding induced changes in DNA conformation, or direct repressor–DNase I interaction.

Repressor binding to the wild-type operator (O_R^+) as a function of pH is shown in Figure 2. Each panel presents the results of multiple, separate experiments. A substantial effect of proton activity is evident. To quantitatively evaluate the effect on the repressor–operator interactions at each of the sites, the total Gibbs energy to saturate each site with ligand was calculated from the data at every condition of pH. This individual-site "loading" energy ($\Delta G_{l,i}$; Ackers et al., 1983) is related to the median ligand activity (X_i; Wyman, 1964) for each of the individual-site isotherms, according to

$$\Delta G_{l,i} = RT \ln X_i = RT \int_0^1 \ln X \, d\, Y_i \quad (3)$$

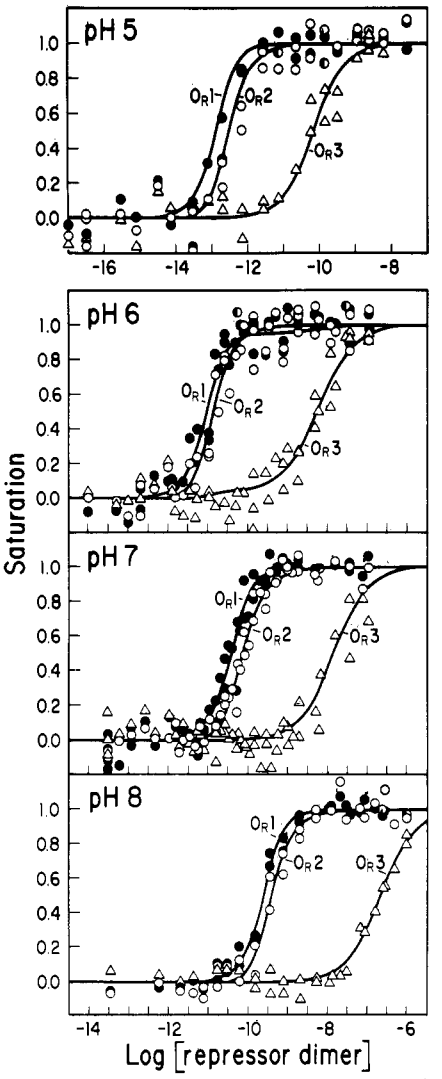

FIGURE 2: Cooperative binding of repressor to O_R versus pH. Reaction conditions are 20 °C, standard assay buffer (200 mM KCl, 1.0 mM $CaCl_2$, and 2.5 mM $MgCl_2$). Panels (from top to bottom) are pH 5, 6, 7, and 8, respectively. Results of several experiments are shown at each condition. Repressor dimer concentrations are calculated as described in the text. (●) Site O_R1; (○) site O_R2; (△) site O_R3. The curves result from simultaneous analysis of binding data for reduced valency mutants, as well as the data shown according to the general cooperativity model, as described in the text. The estimated Gibbs interaction energies are in Table II.

Y_i is the fractional saturation at ligand activity X (e.g., see eq 5 and 6 below).

On the basis of a 1 M *total* repressor standard state, the proton-linked contributions to the individual-site loading energies ($\Delta\Delta G_{1,i}$) over the pH range studied are −2.3, −2.2, and −3.4 kcal/mol for O_R1, O_R2, and O_R3, respectively. Since only repressor dimers bind to operator sites (Pirrotta et al., 1970; Sauer, 1979), these values include a substantial contribution from the free energy to convert a monomer–dimer equilibrium mixture to dimer. Therefore, the data in Figure 2 were plotted and analyzed on the basis of the repressor dimer concentration scale dictated by Sauer's (1979) estimate of the dimer dissociation constant (k_d = 20 nM, under conditions similar to ours) and subject to the simplifying assumption that k_d is pH independent. This treatment of the data is supported by recent measurements of monomer–dimer association free energy (Koblan and Ackers, unpublished experiments) at each of the pH values of this study. The free energy is approximately constant at −11.3 kcal/mol with a range of −11.1 to −11.7 kcal/mol, consistent with the value of −10.4 kcal/mol obtained by Sauer. On this basis, the increase in proton activity changes $\Delta G_{1,1}$, $\Delta G_{1,2}$, and $\Delta G_{1,3}$ by −4.3, −4.1, and −4.6 kcal/mol, respectively.

Comparison of the calculated loading free energies from the separate experiments at each condition of pH provides a model-independent means to assess the reproducibility achieved. The confidence limits for isotherms from single experiments were 0.2–0.3 kcal/mol. In every case, the differences between the calculated values for different experiments at the same conditions were less than or comparable to this, reflecting the lack of any systematic difference. These facts indicate uncertainties of only 0.3–0.4 kcal/mol in the estimation of the $\Delta\Delta G_{1,i}$'s.

Macromolecular Interaction Energies. The Gibbs energy changes for each of the individual macromolecular interactions (i.e., repressor binding and cooperativity) are obtained by analyzing the data using binding expressions which separately consider the individual sites. These are constructed by considering the relative probability, f_s, of each operator configuration:

$$f_s = \frac{\exp(-\Delta G_s/RT)[R_2]^j}{\sum_s \exp(-\Delta G_s/RT)[R_2]^j} \quad (4)$$

where R and T are the gas constant and absolute temperature, respectively, $[R_2]$ is the free repressor dimer concentration, j is the repressor stoichiometry in operator configuration "s", and ΔG_s is the Gibbs energy relative to the unliganded reference state. Simultaneous interaction of the repressor with the three operator sites yields eight possible configurations, detailed in Table I. ΔG_s is given as the sum of contributions of seven microscopic reaction free energies. ΔG_1, ΔG_2, and ΔG_3 denote the intrinsic free energy of binding to each of the operator sites. The remaining terms $[\Delta G_{ij(k)}]$ pertain to the cooperative interactions when repressor is bound simultaneously to two or three sites.[2] These are defined as the difference between the free energy to fill the sites simultaneously (ΔG_T) and the sum of the free energies required to fill them individually, i.e., the sum of the intrinsic binding energies.

The fractional occupancies of each of the operator sites (denoted by Y_i) are given by

$$Y_1 = f_2 + f_5 + f_6 + f_8 \quad (5a)$$

$$Y_2 = f_3 + f_5 + f_7 + f_8 \quad (5b)$$

$$Y_3 = f_4 + f_6 + f_7 + f_8 \quad (5c)$$

Binding expressions for mutant operators in which specific binding to one or more sites has been eliminated are obtained in a similar manner. For example, only configurations 1, 3,

[2] To obtain the most accurate possible values for the intrinsic binding and cooperative energies in each operator configuration, we consider here the most general model for cooperative coupling. This formally considers a unique cooperative interaction energy [denoted by separate $\Delta G_{ij(k)}$ terms] for each multiply liganded operator configuration (lines 5–8, Table I). Previous quantitative analyses of the repressor–O_R interactions have employed the statistical mechanical model presented by Ackers et al. (1982) with only five free energy terms. That model embodies the features of cooperative coupling in O_R proposed by Johnson et al. (1979). These are (i) alternate pairwise cooperativity, which considers cooperative interactions only between adjacent sites, and includes (ii) a "selection" rule, which restricts cooperative interaction to sites O_R1 and O_R2 in the fully saturated repressor. The relationships of the model that employ these constraints to the general formulation presented here, and their application to our data, are discussed in the Appendix.

Table I: Microscopic Configurations and Associated Free Energy Contributions for the λ Repressor–Operator System, O_R[a]

species	operator configurations						free energy contributions
	O_R1		O_R2		O_R3		
1	0		0		0		reference state
2	R_2		0		0		ΔG_1
3	0		R_2		0		ΔG_2
4	0		0		R_2		$\Delta G3$
5	R_2	↔	R_2		0		$\Delta G_1 + \Delta G_2 + \Delta G_{12}$
6	R_2	↔	0	↔	R_2		$\Delta G_1 + \Delta G_3 + \Delta G_{13}$
7	0		R_2	↔	R_2		$\Delta G_2 + \Delta G_3 + \Delta G_{23}$
8	R_2	↔	R_2	↔	R_2		$\Delta G_1 + \Delta G_2 + \Delta G_3 + \Delta G_{123}$
9	R_2	↔	R_2		R_2		$\Delta G_1 + \Delta G_2 + \Delta G_3 + \Delta G_{12}$
10	R_2		R_2	↔	R_2		$\Delta G_1 + \Delta G_2 + \Delta G_3 + \Delta G_{23}$

[a] Individual operator sites are denoted by 0 if vacant or by R_2 if occupied by *c*I repressor dimers. Cooperative interactions are denoted by (↔). ΔG_i values (i = 1, 2, or 3) are the intrinsic Gibbs free energies for binding to each of the three operator sites. $\Delta G_{ij}(k)$ are the free energies of cooperative interaction between liganded sites. The free energies are related to the corresponding microscopic equilibrium constants, k_i, by the standard relationship $\Delta G_i = -RT \ln k_i$. Species 9 and 10 indicate the pairwise cooperative interactions between adjacent operators as proposed by the alternate pairwise model for cooperative interaction in the saturated operator (see Appendix).

4, and 7 (Table I) exist for the O_R1^- operator shown in Figure 1. The binding expressions are

$$Y_1 = 0 \tag{6a}$$

$$Y_2 = f_3 + f_7 \tag{6b}$$

$$Y_3 = f_4 + f_7 \tag{6c}$$

This formulation assumes that the interactions at the remaining site(s) are quantitatively unaffected by the mutation(s).

Cooperativity is evident in the steepness of the transitions for O_R1 and O_R2 (Figures 1 and 2). Separate analysis of the individual O_R^+ titrations according to eq 5 always yielded a minimum variance for $\Delta G_{ij} < 0$ (all experimental conditions). This consistency leads to greater confidence in this result than indicated by the confidence limits for individual experiments which did not exclude $\Delta G_{ij} = 0$ in every case. This later observation is in accord with our previous finding of an asymptotic limit to the shapes of the isotherms for cooperatively coupled binding sites, that is similar to the limiting noncooperative shape (Senear et al., 1986).

To resolve the seven interaction energies, it is necessary to also analyze binding to reduced valency mutants, whose binding competencies are O_R1^-, O_R2^-, $O_R1^-2^-$, and $O_R1^-3^-$. The complete binding data collected for these operators at pH 5 are shown in Figure 3. The data for the different operators were analyzed simultaneously, using the appropriate binding expressions (e.g., eq 5 and 6). Comparison of the O_R2^- and $O_R1^-2^-$ operators indicated $\Delta G_{13} \sim 0$ (see Appendix for discussion). This result was obtained at all pH conditions, and is consistent with earlier reports (Johnson et al., 1979). Therefore, $\Delta G_{13} \equiv 0$ was fixed in the analysis. The results, indicated by the solid curves in the figure, are as follows: $\Delta G_1 = -16.9 \pm 0.3$ kcal/mol, $\Delta G_2 = -14.2 \pm 0.3$ kcal/mol, $\Delta G_3 = -12.3 \pm 0.4$ kcal/mol, $\Delta G_{12} = -2.9 \pm 0.4$ kcal/mol, $\Delta G_{23} = -4.5 \pm 0.5$ kcal/mol, and $\Delta G_{123} = -4.2 \pm 0.7$ kcal/mol.

Proton-Linked Effect. The effect of proton activity on the interaction energies is shown in Figure 4. Resolution of the intrinsic binding energies is excellent, as indicated by the tight confidence limits (error bars in Figure 4) for these parameters. These confidence limits reflect the inherent precision of the binding measurements. The order of repressor affinity, $O_R1 > O_R2 > O_R3$, is maintained over the entire pH range. In particular, note the substantial difference in affinity for O_R2 and O_R3 (from 5- to 25-fold). This difference is well outside the confidence limits for the individual parameters. In this respect, our measurements at 20 °C differ from the earlier estimates at 37 °C (Johnson et al., 1979) which indicated

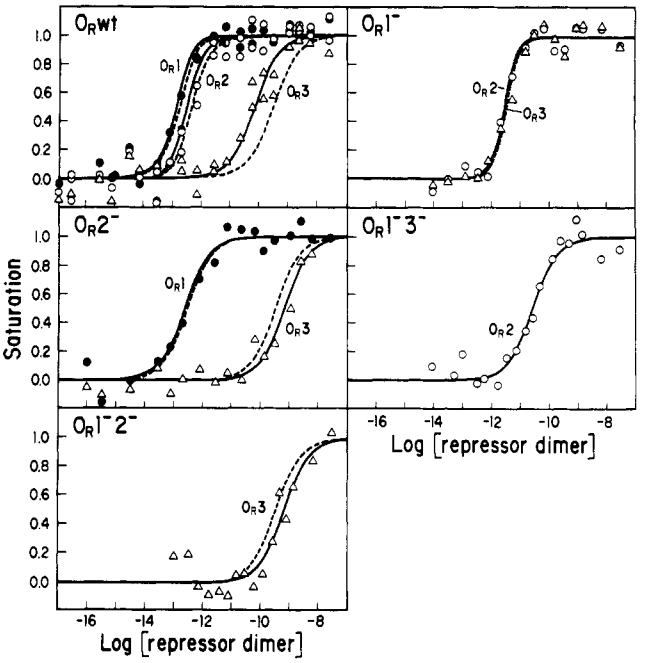

FIGURE 3: Individual-site binding of repressor to O_R^+, and to reduced valency O_R mutants, at pH 5. Operator-containing DNA fragments differ by only 1 bp in each mutated site. Reaction conditions are 20 °C, standard assay buffer. Panels show O_R^+, O_R1^-, $O_R1^-2^-$, and $O_R1^-3^-$ operators, respectively. (●) Site O_R1; (○) site O_R2; (△) site O_R3. The solid curves represent the simultaneous analysis of the data in all panels using the general model described by configurations 1–8 of Table I, and eq 5. Estimated interaction energies are in Table II. The data were also analyzed according to the extended pairwise and alternate pairwise (dashed curves) models (see Appendix). The results are compared in Table V.

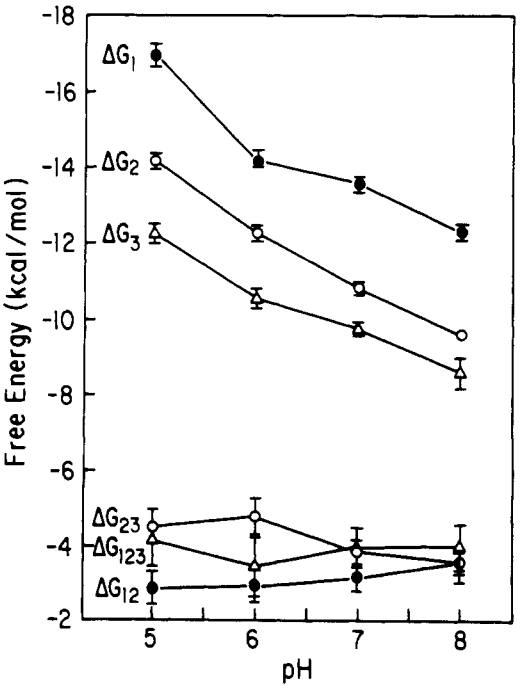

FIGURE 4: Proton-linked effects on free energies of *c*I repressor–O_R interaction at 20 °C, standard conditions. Points plotted are Gibbs energies corresponding to microscopic interaction parameters, resolved by simultaneous analysis of O_R^+ and reduced valency mutant, individual-site binding data as in Figure 3. Error bars represent approximately one standard deviation.

Table II: Proton Linkage of Microscopic Gibbs Energies of Repressor–O_R Interaction[a]

pH	ΔG_1	ΔG_2	ΔG_3	ΔG_{12}	ΔG_{23}	ΔG_{123}	s^b
5	−16.9 ± 0.3	−14.2 ± 0.3	−12.3 ± 0.4	−2.9 ± 0.4	−4.5 ± 0.5	−4.2 ± 0.7	0.087
6	−14.1 ± 0.3	−12.3 ± 0.2	−10.5 ± 0.3	−3.0 ± 0.4	−4.8 ± 0.5	−3.5 ± 0.8	0.103
7	−13.6 ± 0.2	−10.8 ± 0.2	−9.7 ± 0.2	−3.2 ± 0.3	−3.9 ± 0.3	−4.0 ± 0.5	0.071
8	−12.3 ± 0.2	−9.6 ± 0.1	−8.6 ± 0.4	−3.6 ± 0.3	−3.6 ± 0.5	−4.0 ± 0.6	0.062

[a] Standard Gibbs energies (in kilocalories per mole ±65% confidence intervals; 1 cal equals 4.184 J) of the repressor–O_R interactions, obtained by simultaneous analysis of wild-type O_R and reduced valency mutant binding data. Reaction conditions were 20 °C, 200 mM KCl, pH as indicated. [b] Square root of the variance of the fitted curves from the simultaneous analysis.

indentical affinities of repressor for O_R2 and O_R3.

Evaluation of differences between the cooperative free energies is less certain due to slightly greater uncertainty in the values. The confidence intervals for these parameters reflect all systematic differences between separate experiments, and between the different operators, as well as the imprecision of individual experiments. That the estimates are only slightly less precise than the estimates of the intrinsic binding parameters attests to the reproducibility and internal consistency of the data. One difference, that is significant, is a stronger cooperative interaction between O_R2 and O_R3 than between O_R1 and O_R2, at and below neutral pH. This result also differs from the earlier 37 °C result. While the proton-linked effect on the pairwise cooperative free energies is moderate, it is extremely interesting that the direction of the effect differs. Interaction between O_R1 and O_R2 requires net proton absorption, while interaction between O_R2 and O_R3 is accompanied by proton release. ΔG_{123} is essentially constant and generally intermediate between ΔG_{12} and ΔG_{23}. The observation of a smooth trend lends confidence that ΔG_{123} describes a real feature of the repressor–operator interactions, rather than an accumulation of inconsistencies in the binding data.

The proton-linked effect on binding is in the same direction for the three sites and indicates that binding is accompanied by proton absorption. Over the entire range pH 8–5, the magnitude of the effect is of the same order for O_R1 and O_R2, but somewhat less for O_R3. It is important to note the differences in the slopes of the curves in Figure 4. These indicate significant differences in the proton-linked effects at the three operator sites. For example, in the range pH 7 to pH 6, the proton-linked effect on binding to O_R2 is 2–3-fold greater than the effect on binding to either O_R1 or O_R3. Conversely, the effect on binding to O_R1 is half again the effect on binding to O_R2 or to O_R3 in the pH range 6–5. Only in the pH range 7–8 are the effects comparable at all three sites. These differential effects clearly stand above the small uncertainty in the determination of the intrinsic binding parameters.

Discussion

In the present study, we have used the quantitative footprint titration method to assess the proton-linked effects on the interactions of the λ *c*I repressor and O_R. Combined analysis of the isotherms for the wild-type and for several reduced valency mutant operators (Senear et al., 1986) has allowed us to separately resolve the effects on the binding of repressor to each of the operator sites, and on cooperative interactions that arise when repressor binds simultaneously to different operators.

The determinations listed in Table II demonstrate two essential points. First, there is a large proton-linked component to the specific binding of the repressor to its operators. The proton-linked contributions differ by significant amounts between the three sites, indicating differences in the roles of ionizable groups in site-specific recognition. Second, proton-linked contributions to cooperativity are moderate. Here too, the effects on the different cooperative interactions differ. The following discussion will focus on these general features.

Table III: Proton Absorption Linked to *c*I Repressor Binding to O_R[a]

pH	$\Delta\bar{\nu}_H$		
	O_R1	O_R2	O_R3
5.5	2.1 ± 0.3	1.4 ± 0.3	1.3 ± 0.4
6.5	0.4 ± 0.3	1.1 ± 0.2	0.6 ± 0.2
7.5	1.0 ± 0.2	0.9 ± 0.2	0.8 ± 0.3

[a] Net proton absorption ($\Delta\bar{\nu}_H$) upon binding of the *c*I repressor protein to the operator sites of O_R. $\Delta\bar{\nu}_H$, calculated from $\Delta\bar{\nu}_H = \mathrm{d}\ln k/\mathrm{d}\ln a_{H^+} = (1/2.303RT)[\Delta(\Delta G)/\Delta\mathrm{pH}]$, with approximately one standard deviation (by propagation of errors) is shown. The pH reported is the middle of the range for which $\Delta\bar{\nu}_H$ is reported.

Proton-Linked Effects on Repressor Binding. The proton-linked contribution to the free energy of binding to an operator site is equal to the difference $\Delta G_i^{+H} - \Delta G_i^{ref}$, where the superscripts refer to the pH of interest and to a region of high pH in which the free energy is pH independent. From the curves plotted in Figure 5, the highest pH studied, pH 8, does not define a state of complete pH independence. However, it will serve as a useful reference state, from which relative effects, i.e., lower limits to the overall effects, can be calculated. Considering simple differences between the tabulated Gibbs energies shows that the proton-linked effect never accounts for the majority of the binding energy, even at the lowest pH studied. However, by comparing these differences between the three sites, it is clear that proton-linked effects *do* make a major contribution to the differences in binding energy for the three sites. For example, at pH 6, the Gibbs energy for binding to O_R2 is 1.8 kcal/mol more negative than for O_R3. Nearly half of this difference, 0.8 kcal/mol, derives from proton-linked effects. We also note that binding to O_R1 at pH 6 is 1.8 kcal/mol more negative (favorable) than is binding to O_R2, despite a proton-linked contribution that is smaller by 0.9 kcal/mol.

The uncertainties reported in Table II represent worst case joint confidence limits (see Materials and Methods; Johnson & Frasier, 1985) which present a conservative view of the precision obtained. Usually, the data exclude numerical solutions with any two parameters at the confidence limit values. This fact, and the reproducibility achieved from multiple determinations of the same isotherms, causes us to place great confidence in these statistically significant differences.

Number of Linked Protons. The slopes of the curves plotted in Figure 4 are related to net proton absorption, according to $\Delta\bar{\nu}_H = \mathrm{d}\ln k/\mathrm{d}\ln a_H$ (Wyman, 1964), where k is the microsocpic association equilibrium constant. Fitting the data to an arbitrary smooth function that closely matches its trends is usually the best way to compute derivatives. However, the number of pH values from which the interaction free energies were determined justifies a simpler approach. Therefore, $\Delta\bar{\nu}_H$ was calculated by differences between pairs of free energy determinations, according to $\Delta\bar{\nu}_H = (1/2.303RT)[\Delta(\Delta G)/\Delta\mathrm{pH}]$. The values estimated for the binding reactions are in Table III.

At all three operators, repressor binding is accompanied by

proton absorption. This reflects a shift in pK_a's of ionizable groups toward more basic values, and is in the expected direction for the response of a mildly acidic protein (Sauer, 1979) to binding to polyanionic DNA. It seems unlikely that titration of the DNA is involved in the observed proton-linked effects. Though dramatic pK_a shifts have been observed for certain copolymer DNA sequences [cf. Hartman and Rich (1965)], extensive titration data for eukaryotic DNAs [cf. Cox and Peacock (1956) and references cited therein] confirm the lack of proton binding by mixed-sequence DNA over the pH range studied. Therefore, we conclude that amino acid side chains of the repressor are responsible for the proton-linked effects.

Clear patterns of $\Delta\bar{\nu}_H$ versus pH are observed. These patterns provide a clue to the ionizable groups that might be involved. In particular, we note that $\Delta\bar{\nu}_H$ for O_R2 is nearly constant (and large) over the entire pH range, while $\Delta\bar{\nu}_H$ for O_R1 and O_R3 are large at the extremes, but more moderate between pH 6 and pH 7. This pattern requires pK_a shifts of at least two groups, one titrating (in free repressor) near pH 5 and a second perhaps near pH 7. It seems most likely that the observed effects reflect the cumulative result of small effects on several ionizable groups.

Assignment of Effects. The repressor NH_2-terminal domain/O_L1 cocrystallographic structure (Jordan & Pabo, 1988) indicates no ion pair type interactions, and no H-bond interactions which involve acidic or neutral groups on the repressor. Therefore, the site-specific proton-linked effects observed do not reflect a direct readout of differences in DNA sequence between the operator sites. Instead, we envision these effects as arising in either of two ways. First, the observed DNA sequence-dependent variations in the backbone phosphate conformation/orientation might cause sufficient variation in the electrostatic potential surfaces of the various operator sites to be felt as direct electrostatic effects by ionizable groups on the repressor. Second, any conformational accommodation of the repressor to site-specific differences in the DNA conformation might lead indirectly to differential pK_a shifts.

The small number of ionizable groups on the DNA binding surface of the repressor NH_2-terminal domain and the absence of histidine and cystine (Sauer & Anderegg, 1978) tempt us to speculate regarding the groups that might be responsible for observed effects. The crystal structure points to two intriguing possibilities. First is Glu-34, located on the DNA binding interface of helix 2. Different side chain orientations in the subunits interacting with the consensus and nonconsensus operator half-sites are related by a rotation of approximately 90° around the $^{\alpha}C$–$^{\beta}C$ bond. The carboxylate oxygens of Glu-34 and the phosphate oxygens of adenosine at position −1 on the 5′ strand of the consensus half-site are in van der Waals contact (this phosphate does not show protection in ethylation interference experiments; Johnson, 1980). In the nonconsensus half-site, these carboxylate oxygens are located above the major groove of the DNA, about 10 Å from the nearest phosphate oxygens. This difference must yield different pK_a's for Glu-34 in the two subunits of bound repressor. Similar conformational effects might also yield different pK_a's for repressor interacting with the different half-site in different operators.

Second is the terminal amino group, one of only very few groups that might account for neutral to slightly basic pK_a values. The NH_2-terminal arm of the repressor has been shown to be critical to site-specific recognition (Nelson et al., 1983; Hecht et al., 1983; Eliason et al., 1986; Nelson & Sauer, 1986). The crystal structure confirms previous biochemical evidence, placing the arm in the major groove of the DNA, on the backside and toward the center of the operator site. While the terminal NH_2 is not in intimate contact with any backbone phosphate, the crystal structure does indicate some disorder in the structure of the NH_2-terminal arm, and possible differences between the two subunits.

Table IV: Individual-Site Loading Free Energies for Mutant Operators O_R2^- and $O_R1^{r}2^{-}$[a]

	O_R2^- operator		$O_R1^{r}2^-$ operator[b]	
pH	$\Delta G_{1,1}$	$\Delta G_{1,3}$	$\Delta G_{1,1}$	$\Delta G_{1,3}$
5	−16.8 ± 0.3	−12.2 ± 0.5	−13.5 ± 0.2	−12.3 ± 0.4
6[c]	−14.0 ± 0.3	−10.4 ± 0.3	−11.5 ± 0.2	−10.6 ± 0.2
7	−13.3 ± 0.3	−10.0 ± 0.8	−10.7 ± 0.2	−9.7 ± 0.3
8	−12.3 ± 0.2	−8.8 ± 0.4	−9.1 ± 0.2	−8.4 ± 0.3

[a] Gibbs loading energies for sites O_R1 ($G_{1,i}$) and O_R3 ($G_{1,3}$) representing the total chemical work to saturate each operator site. Calculation of $G_{1,i}$ and the confidence limits are described in the text. Experiments were conducted in assay buffer (see text) with pH as indicated. Values listed are in kilocalories per mole. [b] Operator designation 1^r refers to the v3 mutation of O_R1 (Meyer et al., 1979) which reduces repressor affinity by ca. 1000-fold. [c] Data shown in Figure 5.

Proton-Linked Effects on Cooperativity. Interpretation of the proton-linked effects on cooperativity is less certain, both because the resolution of the Gibbs energies is less precise (Table II) and because of high correlation between those parameters and the energy of repressor dimer dissociation. Despite this, it is clear that while the Gibbs energies of cooperative interaction between O_R1 and O_R2, and between O_R2 and O_R3, are nearly identical at and above neutral pH (in agreement with previous studies; Ackers et al., 1982), they are quite distinguishable in the acid pH range. Thus, O_R2–R_R3 cooperativity features greater net proton absorption than O_R1–O_R2 cooperativity, indicating coupling between the cooperative mechanisms, and site-specific binding. This result suggests an obligatory communication between the carboxy-terminal domain that mediates cooperativity, and the NH_2-terminal domain that binds DNA. This is consistent with the finding that removal of the carboxy-terminal domain reduces the operator affinity of the repressor by several orders of magnitude (Johnson et al., 1979).

Pattern of Cooperative Coupling. The extensive, internally consistent data base generated by these studies has allowed critical evaluation of previously proposed statistical–thermodyanamic models for the pattern of cooperative coupling in O_R. These issues are discussed in the Appendix. The data confirm the assumption (Johnson et al., 1979; Maurer et al., 1980) of no significant coupling interaction between liganded operators O_R1 and O_R3. This implies that cooperativity involves direct coupling between operators, rather than long-range structural perturbations of the DNA. The data in the acid pH range are inconsistent with a rule (Johnson et al., 1979) that pairwise cooperative interaction between O_R1 and O_R2 is only possible in the absence of ligation of O_R1. There appears to be no special mechanism of coupling to O_R1 binding that precludes participation of O_R3 under the conditions of this study. The data do not distinguish between the extended pairwise and general models of cooperativity, which appear to be numerically equivalent at the conditions studied. In the absence of clear evidence, both thermodynamic and otherwise, that only pairwise interaction is possible, we choose to analyze our data according to the more general model, preferring not to place a priori constraints on the data.

It was the observation that the apparent affinity of O_R3 for repressor is increased severalfold by mutation of O_R1 (Johnson et al., 1979) which led to the proposal of the special selection rule. Our data (which confirm the above observation at all

conditions) provide a simple explanation. Since the occupancy of O_R3 is near zero until O_R1 and O_R2 approach saturation (Figure 2), the apparent free energy to load O_R3 is approximately $\Delta G_3 + \Delta G_{123} - \Delta G_{12}$. This is the difference in Gibbs free energies between species 5 and 8 of Table I. Since ΔG_{12} and ΔG_{123} differ by a small amount at pH 7 and above, this is approximately equal to ΔG_3. By contrast, O_R2 and O_R3 fill together in an O_R1^- operator (Figure 3), and $\Delta G_{1,3} = \Delta G_3 + f(\Delta G_{23})$. Since O_R3 has lower intrinsic affinity by 1–2 kcal/mol (Table IV), the cooperative energy is primarily "felt" by O_R3 (Ackers et al., 1983) so that the fraction, f, is near unity, yielding approximately $\Delta G_3 + \Delta G_{23}$. Thus, the observation cited is a necessary consequence of the different operator affinities, and of the similar cooperative energies at pH 7 and not an indication of alternate pairwise coupling.

Concluding Remarks. Recent crystallographic evidence has challenged the long-held view that site-specific recognition of DNA by regulatory proteins is solely due to direct interaction, primarily by H-bonding and van der Waals interactions, with the exposed edges of the base pairs in the major groove of the DNA. For example, the *E. coli* tryptophan repressor is highly specific without such interactions (Otwinowski et al., 1988).

Many mutational studies of the recognition helix of the λ repressor and of the operator sequences have been interpreted in terms of simple, direct contacts. However, the λ repressor/O_L crystallographic structure (Jordan & Pabo, 1988) is inconsistent with this simplistic view. Specific contacts are detected with only 3 of the 8 bp per operator half-site. These are A·T at position 2 and C·G at positions 4 and 6. Specific contacts with these base pairs, which are the only highly conserved base pairs in both consesus and nonconsensus half-sites (i.e., 35 out of 36 occurences), are undoubtedly crucial in discriminating between operator and nonoperator sequences. However, these interactions cannot explain the differential affinity of repressor for its three operator sites at O_R (and at O_L), a crucial feature of the lysogenic–lytic switch mechanism. We note that the affinity difference between O_R1 and O_R3 (ca. 4 kcal/mol or 1000-fold at all conditions we have studied) is greater than the affinity difference between O_R3 and nonoperator DNA (Senear, unpublished observations).

In contrast to the structural studies, recent exhaustive mutagenesis studies have identified six base pairs as crucial to recognition (Benson & Youderian, 1989) in vivo. The additional base pairs identified by the in vivo studies are at positions (5, 7, and 8) where both the structural studies and ethylation interference experiments (Johnson, 1979) implicate interactions with backbone phosphates. Other recent mutagenesis experiments (Hochschild & Ptashne, 1988) have confirmed the role of the base pair at position 5 in the nonconsensus half-site as being involved in the ability of repressor to discriminate O_R1 from O_R3.

That interactions with the deoxyribose–phosphate backbone should be important in site-specific binding clearly implicates a role for the sequence-dependent conformation of the DNA. This provides a potential explanation for our recent observation that the DNA sequence flanking the operator sites can cause 10-fold changes in operator affinity (Brenowitz et al., 1989). The thermodynamic data presented here further demonstrate how groups that do not physically contact one another can be involved in the repressor–operator interactions. Thus, both direct reading and indirect reading of the DNA sequence are necessary to the cooperative, site-specific interactions of the repressor and its operators. Repressor proteins and DNA operators need both be viewed as interacting macromolecules, whose preferred three-dimensional structures are crucial to complex formation and to biological regulation. Both structural and thermodynamic studies, in addition to molecular genetic and molecular biological studies, will be necessary to understand regulation in these complexes.

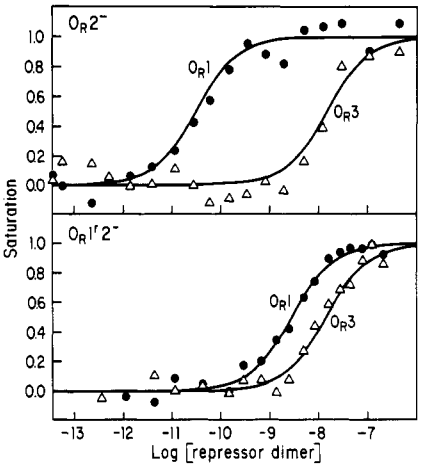

FIGURE 5: Comparison of individual-site isotherms for repressor binding to reduced valency operators, to evaluate cooperative interaction between sites O_R1 and O_R3. The DNA fragments (1107 bp) differ from the wild-type sequence by 1 bp in each mutated site. The reaction conditions are 20 °C, standard assay buffer, pH 6. The top and bottom panels show O_R2^- and $O_R1^r2^-$ operators, respectively (where "1r" refers to reduced, but not eliminated, specific affinity for O_R1). (●) Site O_R1; (△) site O_R3. Individual-site loading energies, calculated by numerical integration of these data, are in Table IV. The solid curves are the noncooperative binding curves corresponding to those loading energies.

Appendix

The configurations listed in lines 1–8 of Table I present the most general model for cooperative interaction between three DNA operator sites. Each configuration with more than one occupied site is described by a unique coupling or cooperative energy [$\Delta G_{ij(k)}$]. Johnson et al. (1979) proposed specific features of cooperative interaction in the λ operators, based on their semiquantitative estimation of repressor concentrations needed to half-saturate the operator sites of O_R, and of reduced valency mutants. These features yield rules which constrain our general model. The rules are (1) no cooperative interaction between sites 1 and 3, (2) cooperative interaction is strictly pairwise, and (3) no cooperative interaction between O_R2 and O_R3 when O_R1 is liganded.

The statistical mechanical formulation of these rules is straightforward. Rule 1 specifies $\Delta G_{13} = 0$. Rule 2 leads to the replacement of species 8 in Table I, by species 9 and 10. It dictates the functional dependence $\Delta G_{123} = -RT \ln [\exp(-\Delta G_{12}/RT) + \exp(-\Delta G_{23}/RT)]$. Rule 3 further eliminates species 10 to give $\Delta G_{123} = \Delta G_{12}$. As discussed previously (Senear et al., 1986), high statistical correlation precludes unique resolution of ΔG_2 and of the $\Delta G_{ij(k)}$ terms for any of these three possible coupling models (which we refer to as general, extended pairwise, and alternate pairwise) from individual-site isotherms for O_R^+ alone. This necessitates reliance on comparisons between O_R^+ and reduced valency mutants to resolve coupling constants according to any of the models, or to discriminate differences between the three models. Of course, such comparisons rely on the assumption that single base pair substitutions in the mutated sites produce no intrinsic effect on the remaining sites.

In the studies presented here, we have generated complete individual-site isotherms for O_R^+ and for several reduced valency mutant operators over a range of experimental conditions. These data present the first opportunity to critically evaluate rules 1–3 as formulated in the different coupling

models, while simultaneously evaluating the validity of the comparisons between mutant operators. We presume that only a combination of reduced valency mutants that behave according to our assumption and a correct coupling model will combine to give internally consistent results over a wide range of experimental conditions.

Rule 1: Cooperative Interaction between O_R1 and O_R3. Figure 5 compares individual-site isotherms for two operators in which specific binding to O_R2 has been eliminated. One operator also contains the v3, C → A mutation in O_R1 (Meyer et al., 1980) reported to eliminate specific binding. It is clear from the figure that specific binding is not eliminated though repressor affinity is reduced by ca. 1000-fold. The appreciable remaining, specific repressor binding affinity at O_R1 (O_R1^r) invalidates the previous simple comparison between the half-saturation points for O_R3 (Johnson et al., 1979) to evaluate cooperative interaction between O_R1 and O_R3. ΔG_{13} is not simply the difference in apparent binding energies for O_R3, as it would be, were the second operator actually $O_R1^-2^-$.

A model-independent evaluation of ΔG_{13} is still possible, by quantitative comparison of the individual-site loading energies ($\Delta G_{1,i}$) for the four isotherms. These are listed for each pH in Table IV. $\Delta G_{1,i}$ represents the total chemical work to saturate site i, including a partial contribution from all cooperative interactions involving site i [i.e., $\Delta G_{ij(k)}$]. Partitioning of ΔG_{ij} between $\Delta G_{1,i}$ and $\Delta G_{1,j}$ is strongly dependent on the relative affinities of the two sites (see Figure 5; Ackers et al., 1983). If $|\Delta G_{1,i} - \Delta G_{1,j}| \gg |\Delta G_{12}|$, then two titration isotherms do not overlap, and cooperativity is primarily "felt" by the weaker site. This is the case for the top panel of Figure 5, so that $\Delta G_{1,1} \sim \Delta G_1$ and $\Delta G_{1,3} \sim \Delta G_3 + \Delta G_{13}$. However, this is not the case for the data in the bottom panel. There, $\Delta G^r_{1,1} = \Delta G^r_1 + f\Delta G_{13}$ and $\Delta G_{1,3} = \Delta G_3 + (1 - f)\Delta G_{13}$, where $0.5 \geq f \geq 0$. Thus, we expect $\Delta G_{1,3}$ to differ for the two operators by the quantity $f\Delta G_{13}$, where f may be small. In fact, comparing columns 2 and 4 of Table IV shows $|f\Delta G_{13}|$ to be zero on average, subject to ±0.3 kcal/mol of experimental uncertainty.

From these values, we calculate an upper limit to $|\Delta G_{13}|$ as follows. For two-site operators, analytical expressions of the form $\Delta G_{1,i} = f(\Delta G_i, \Delta G_j, \Delta G_{ij})$ have been derived (Ackers et al., 1983). Their application to the data in Table IV produces a system of four nonlinear equations with parameters ΔG_1, ΔG_3, ΔG_{13}, and ΔG^r_1. This system of equations was solved numerically, taking the mean difference observed for $\Delta G_{1,3}$ (+0.1 kcal/mol) plus one standard deviation (0.3 kcal/mol) as being the maximum possible difference. The calculation yields $\Delta G_{13} \geq -0.8$ kcal/mol. This energy appears insignificant when compared to the cooperative interaction between adjacent sites (Table II) and by its effect on the population distribution of operator configurations.

Rules 2 and 3: Cooperative Interaction in Fully Liganded O_R. To address this issue, the individual-site binding data for the O_R^+, O_R1^-, O_R2^-, $O_R1^r2^-$, and $O_R1^-3^-$ operators were simultaneously analyzed according to the general, extended pairwise, and alternate pairwise models described above. The results of these analyses for the data collected at pH 5 are presented in Figure 3. On the basis of the conclusion from the previous section, $\Delta G_{13} = 0$ was fixed in all analyses, and the titration of O_R1 in the $O_R1^r2^-$ operator was ignored.

In previous comparisons of wild-type and mutant isotherms, we have based our argument for the validity of the comparison based on the internal consistency of the isotherms, as indicated by agreement of the model parameters obtained for all combinations of operators (Senear et al., 1986). Since we now face the additional interrelated issue of evaluating different coupling models, we base our argument on a more rigorous criterion, one which also accounts for the information provided by the detailed shapes of the individual-site isotherms. We now require that simultaneous analysis according to the "correct" coupling model produces isotherms for each operator that are within the confidence envelopes of the isotherms obtained as the best phenomenological fit to each of the separate operators. We use an F statistic (Box, 1960) to define the variance ratio corresponding to the limits of these confidence envelopes and require an essentially random distribution of residuals for each isotherm.

Table V: Microscopic Free Energies of Interaction for cI Repressor Binding to O_R at pH 5, Estimated According to Different Coupling Models[a]

interaction energy	cooperativity model		
	general	extended pairwise	alternate pairwise
ΔG_1	−16.9 ± 0.3	−16.7 ± 0.4	−16.8 ± 0.4
ΔG_2	−14.2 ± 0.2	−14.2 ± 0.3	−14.2 ± 0.3
ΔG_3	−12.3 ± 0.3	−12.3 ± 0.3	−12.7 ± 0.3
ΔG_{12}	−2.9 ± 0.4	−2.6 ± 0.6	−2.6 ± 0.6
ΔG_{23}	−4.5 ± 0.5	−4.0 ± 0.7	−4.0 ± 0.6
ΔG_{123}	−4.2 ± 0.7		
S^b	0.087	0.088	0.097

[a] Standard Gibbs energies (with 65% confidence intervals) for the data of Figure 4. The interaction energies are defined in Table I for three different mechanisms for cooperative interaction in the saturated operator. The general, extended pairwise, and alternate pairwise are defined by configurations 1–8, 1–7 plus 9–10, and 1–7 plus 9 in Table I, respectively. Binding expressions are derived by using eq 2 as described in the text. All values reported are kilocalories per mole. [b] Square root of the variance of the fitted curves.

The microscopic interaction energies obtained by these analyses for the pH 5 data are listed in Table V. The parameters from the three models are similar, differing primarily by small amounts in the $\Delta G_{ij(k)}$ terms, which are generally not statistically meaningful. Despite this, the goodness of fit varies markedly between the different models, as indicated by an appreciably greater variance (sigma) for the alternate pairwise model than for the general and extended pairwise models.

As illustrated by the curves in Figure 3, the difference in σ values substantially understates the difference in goodness of fit. This is because the increase arises from only a subset of the data. The isotherms pertaining to the general model (solid lines) compare favorably to the best phenomenological curves for the individual operators (for simplicity, the substantially identical isotherms pertaining to the extended pairwise model are not shown). This excellent correspondence argues strongly that the mutations in these operators do not perturb the interactions at the remaining sites. By contrast, the isotherms pertaining to the alternate pairwise model (dashed lines) deviate substantially and systematically from the O_R3 binding data in the O_R^+, O_R2^-, and $O_R1^-2^-$ operators. The reason for this difference is that the cooperative energy in the triply liganded operator that is dictated by the data (−4.2 kcal/mol) does not equal ΔG_{12}, in violation of the constraint imposed by this model. However, the constraint imposed by the extended pairwise model is satisfied.

Results at the other pH values are similar. The intrinsic binding energies resolved by the different models are substantially the same, obviating concerns regarding the influence of the coupling model on the interpretation of proton-linked effects. This fact primarily reflects the dominant influence of the noncooperative sites of the $O_R1^-2^-$, $O_R1^-3^-$, and O_R2^-

operators in determining the ΔG_i values. The general model always gives a better description than the extended pairwise model with the major differences found primarily in the O_R1 isotherms. The significance is difficult to assess, given the noise of the data. Therefore, while the data do not eliminate this model, they provide little support for it. The alternate pairwise model is easily eliminated by the systematic deviations from the O_R3 data.

References

Ackers, G. K., Johnson, A. D., & Shea, M. A. (1982) *Proc. Natl. Acad. Sci. U.S.A. 79*, 1129–1133.

Ackers, G. K., Shea, M. A., & Smith, F. N. (1983) *J. Mol. Biol. 170*, 223–242.

Aggarwal, A. K., Rodgers, D. W., Drotlar, M., Ptashne, M., & Harrison, S. C. (1988) *Science 242*, 899–907.

Backman, K., Ptashne, M., & Gilbert, W. (1976) *Proc. Natl. Acad. Sci. U.S.A. 73*, 4174–4178.

Benson, N., Sugiono, P., & Youderian, P. (1988) *Genetics 118*, 21–29.

Bevington, P. R. (1969) *Data Reduction and Error Analysis for the Physical Sciences*, McGraw-Hill, New York.

Birnboim, H., & Doly, J. (1979) *Nucleic Acids Res. 7*, 1513–1523.

Box, G. D. P. (1960) *Ann. N.Y. Acad. Sci. 86*, 792.

Brenowitz, M., Senear, D. F., Shea, M. A., & Ackers, G. K. (1986a) *Proc. Natl. Acad. Sci. U.S.A. 83*, 8462–8466.

Brenowitz, M., Senear, D. F., Shea, M. A., & Ackers, G. K. (1986b) *Methods Enzymol. 130*, 132–181.

Brenowitz, M., Senear, D. F., & Ackers, G. K. (1989) *Nucleic Acids Res. 17*, 3747–3755.

Cox, R. A., & Peacock, A. R. (1956) *J. Chem. Soc.*, 2499–2512.

Eliason, J. L., Weiss, M. A., & Ptashne, M. (1985) *Proc. Natl. Acad. Sci. U.S.A. 82*, 2339–2343.

Hartman, K., & Rich, A. (1965) *J. Am. Chem. Soc. 87*, 2033.

Hecht, M. H., Nelson, H. C. N., & Sauer, R. T. (1983) *Proc. Natl. Acad. Sci. U.S.A. 80*, 2676–2680.

Hildebrand, F. B. (1956) *Introduction to Numerical Analysis*, McGraw-Hill, New York.

Hill, T. L. (1960) *Introduction to Statistical Thermodynamics*, Addison Wesley, Reading, MA.

Hochschild, A., Douhan, J., & Ptashne, M. (1986) *Cell 47*, 807–816.

Johnson, A. D. (1980) Ph.D. Dissertation, Harvard University, Cambridge, MA.

Johnson, A. D., Meyer, B. J., & Ptashne, M. (1979) *Proc. Natl. Acad. Sci. U.S.A. 76*, 5061–5065.

Johnson, L. W., & Riess, R. D. (1982) *Numerical Analysis*, Addison-Wesley Publishing Co., Reading, MA.

Johnson, M. L., & Frasier, S. G. (1985) *Methods Enzymol. 117*, 301–342.

Jordan, S. R., & Pabo, C. O. (1988) *Science 242*, 893–899.

Kunitz, M. (1950) *J. Gen. Physiol. 33*, 349.

Maniatas, T., Fritsch, E. F., & Sambrook, J. (1982) *Molecular Cloning—A Laboratory Manual*, Cold Spring Harbor Laboratory, Cold Spring Harbor, NY.

Maurer, R., Meyer, B. J., & Ptashne, M. (1980) *J. Mol. Biol. 138*, 147–161.

Meyer, B. J., Maurer, R., & Ptashne, M. (1980) *J. Mol. Biol. 139*, 163–194.

Nelson, H. C. M., & Sauer, R. T. (1986) *J. Mol. Biol. 192*, 27–38.

Nelson, H. C. M., Hecht, M. H., & Sauer, R. T. (1983) *Proc. Natl. Acad. Sci. U.S.A. 80*, 2676–2680.

Ptashne, M. (1986) *The Genetic Switch*, Cell Press, Cambridge, MA.

Sauer, R. (1970) Ph.D. Dissertation, Harvard University, Cambridge, MA.

Sauer, R. T., & Anderegg, R. (1978) *Biochemistry 17*, 1092–1100.

Senear, D. F., Brenowitz, M., Shea, M. A., & Ackers, G. K. (1986) *Biochemistry 25*, 7344–7354.

Shea, M. A., & Ackers, G. K. (1983) in *Mobility and Recognition in Cell Biology* (Sund, H., & Veeger, C., Eds.) de Gruyter, Berlin.

Ward, B., Rehfuss, R., Goodisman, J., & Dabrowiak, J. C. (1988) *Biochemistry 27*, 1198–1205.

Wolberger, C., Dong, Y., Ptashne, M., & Harrison, S. C. (1988) *Nature 335*, 789–795.

Wyman, J., Jr. (1964) *Adv. Protein Chem. 19*, 224–394.